

# Dynamics of the phase separation in a thermoresponsive polymer: accelerated phase separation of stereo-controlled poly(N,N-diethylacrylamide) in water

メタデータ	<p>言語: English</p> <p>出版者: ACS Publications</p> <p>公開日: 2019-11-01</p> <p>キーワード (Ja): 温度応答性高分子, 相分離ダイナミクス, レーザー温度ジャンプ法, 立体規則性, コイル-グロビュール相転移</p> <p>キーワード (En): Thermoresponsive polymer, Phase separation dynamics, Laser T-jump technique, Tacticity, Coil-to-globule phase transition</p> <p>作成者: 松本, 充央, 多田, 貴則, 麻生, 隆彬, 東海林, 竜也, 西山, 聖, 堀邊, 英夫, 勝本, 之晶, 坪井, 泰之</p> <p>メールアドレス:</p> <p>所属: Osaka City University, Osaka City University, Osaka City University, Hokkaido University, Osaka City University, Osaka City University, Osaka City University, Osaka City University, Fukuoka University, Osaka City University, Hokkaido University</p>
URL	<p><a href="https://ocu-omu.repo.nii.ac.jp/records/2020051">https://ocu-omu.repo.nii.ac.jp/records/2020051</a></p>

# Dynamics of the Phase Separation in a Thermoresponsive Polymer: Accelerated Phase Separation of Stereocontrolled Poly(*N,N*-diethylacrylamide) in Water

Mitsuhiro Matsumoto, Takanori Tada, Taka-Aki Asoh, Tatsuya Shoji, Takashi Nishiyama, Hideo Horibe, Yukiteru Katsumoto, Yasuyuki Tsuboi

<b>Citation</b>	Langmuir, 34 (45); 13690–13696
<b>Issue Date</b>	2018-10-26
<b>Type</b>	Journal Article
<b>Textversion</b>	author
<b>Rights</b>	This document is the Accepted Manuscript version of a Published Work that appeared in final form in Langmuir, copyright © American Chemical Society after peer review and technical editing by the publisher. To access the final edited and published work see <a href="https://doi.org/10.1021/acs.langmuir.8b02848">https://doi.org/10.1021/acs.langmuir.8b02848</a>
<b>DOI</b>	10.1021/acs.langmuir.8b02848

Self-Archiving by Author(s)  
Placed on: Osaka City University

1  
2  
3  
4  
5  
6  
7 Dynamics of the phase separation in a  
8  
9  
10  
11 thermoresponsive polymer: accelerated phase  
12  
13  
14  
15 separation of stereo-controlled poly(*N,N*-  
16  
17  
18  
19 diethylacrylamide) in water  
20  
21  
22  
23

24 *Mitsuhiro Matsumoto*<sup>a</sup>, *Takanori Tada*<sup>b</sup>, *Taka-Aki Asoh*<sup>a,c</sup>, *Tatsuya Shoji*<sup>a</sup>, *Takashi Nishiyama*  
25  
26 *<sup>d</sup>*, *Hideo Horibe*<sup>d</sup>, *Yukiteru Katsumoto*<sup>e</sup>, *Yasuyuki Tsuboi*<sup>a,c\*</sup>  
27  
28

29 a. Division of Molecular Materials Science, Graduate School of Science, Osaka City University,  
30  
31 3-3-138 Sugimoto, Sumiyoshi, Osaka 558-8585, Japan  
32  
33

34 b. The Osaka City University Advanced Research Institute for Natural Science and Technology  
35  
36 (OCARINA), Osaka City University, 3-3-138, Sugimoto, Sumiyoshi, Osaka, 558-8585 Japan  
37  
38

39 c. Graduate School of Chemical Sciences and Engineering, Hokkaido University, Sapporo 060-  
40  
41 0810, Japan  
42  
43

44 d. Department of Applied Chemistry and Bioengineering, Graduate School of Engineering,  
45  
46 Osaka City University, 3-3-138 Sugimoto, Sumiyoshi, Osaka 558-8585, Japan  
47  
48

49 e. Department of Chemistry, Faculty of Science, Fukuoka University, 8-19-1 Nanakuma, Jonan-  
50  
51 ku 814-0180, Japan  
52  
53  
54  
55  
56  
57  
58  
59  
60

1  
2  
3 **ABSTRACT:** We studied the dependence on tacticity of the dynamic phase separation behavior  
4 of thermoresponsive poly(*N,N*-diethylacrylamide) (PDEA) in an aqueous solution. Using a laser  
5 temperature-jump technique combined with transient photometry, we determined the time  
6 constants of the phase separation, and found that both atactic and isotactic-rich PDEAs had fast  
7 and slow phase separation processes ( $\tau_{\text{fast}}$  and  $\tau_{\text{slow}}$ ). The fast process ( $\tau_{\text{fast}}$ ) was independent of  
8 the tacticity irrespective of the concentration. On the other hand, the slow process had a strong  
9 dependence on the tacticity. We found the slow phase separation process got considerably faster  
10 with increasing isotacticity in dilute solutions. This effect due to the tacticity of the PDEA is  
11 totally different from that for poly(*N*-isopropylacrylamide) and can be explained based on the  
12 difference between the hydrophobicity of atactic PDEA and that of isotactic-rich PDEA.  
13  
14  
15  
16  
17  
18  
19  
20  
21  
22  
23  
24  
25  
26  
27  
28  
29  
30  
31  
32  
33  
34  
35  
36  
37  
38  
39  
40  
41  
42  
43  
44  
45  
46  
47  
48  
49  
50  
51  
52  
53  
54  
55  
56  
57  
58  
59  
60

## Introduction

In 1968, Heskins and Guillet reported the first demonstration of an aqueous solution of poly(*N*-isopropylacrylamide) (PNIPAM) exhibiting reversible phase separation with lower critical solution temperature (LCST).<sup>1</sup> Following this discovery, the fundamental features of PNIPAM were investigated by static/dynamic light scattering,<sup>2–7</sup> vibrational spectroscopy,<sup>6,8–10</sup> NMR spectroscopy,<sup>11,12</sup> calorimetry,<sup>13–15</sup> small-angle neutron scattering,<sup>16,17</sup> and so on. These numerous studies show that PNIPAM chains are homogeneously dissolved in water below the LCST taking hydrated random-coil structures. Upon heating above the LCST, the PNIPAM chains turn into globular structures accompanied by dehydration of the polymer chains (coil-to-globule phase transition). Subsequently, these dehydrated polymer chains (globules) aggregate with each other. Finally, the solution separates into water-rich and polymer-rich-domains due to hydrophobic interactions between the globules (phase separation). Until now, many researchers have synthesized a number of LCST-type thermoresponsive polymers such as poly(*N*-substituted acrylamide)s, poly(*N*-substituted methacrylamide)s, and poly(alkyl vinyl ether)s.<sup>18,19</sup>

In addition to PNIPAM, poly(*N,N*-diethylacrylamide) (PDEA) is another representative LCST-type thermoresponsive polymer. PDEA has an analogous chemical structure to PNIPAM, and both polymers have similar LCSTs. PDEA has been studied to understand the dependence of the phase separation behavior on the chemical structure.<sup>20,21,30–38,22–29</sup> For instance, Itakura et al. and Zhang et al. reported that PDEA partly formed precursory polymer aggregates in a dilute aqueous solution even below the LCST.<sup>21,22</sup> For PNIPAM, such precursory polymer aggregates have never been observed. Furthermore, Maeda et al. and Hashimoto et al. spectroscopically investigated PDEA and suggested that the side chains of PDEA were more hydrophobic than those of PNIPAM.<sup>23,24</sup> Not only these static properties but also the dynamic properties of the

1  
2  
3 phase separation behavior (phase separation dynamics) are important to further understand the  
4 effect of the side chains. Recently, we investigated the phase separation dynamics for PDEA  
5 using a method previously developed by us that combines a laser temperature-jump (T-jump)  
6 technique with transient photometry.<sup>39</sup> In a previous study we showed that the phase separation  
7 for PDEA is much faster than that for PNIPAM, and the phase separation mechanism for PDEA  
8 is partly different from that for PNIPAM.<sup>40</sup> Such obvious differences between PNIPAM and  
9 PDEA are due to interactions between the side chains and water molecules and/or between the  
10 side chains themselves (hydrophobic interaction).<sup>41</sup>

11  
12 In the present study, we focused on the tacticity of PDEA. In 2000, Nakahama et al  
13 synthesized both highly isotactic and highly syndiotactic PDEA by anionic polymerization and  
14 found that highly syndiotactic PDEA did not dissolve in water.<sup>42</sup> Furthermore, Katsumoto et al.  
15 reported on the effect of the tacticity on the phase diagram and presented hydration structures for  
16 both aqueous PDEA solutions and thin PDEA films.<sup>41,43</sup> These studies indicate that isotactic-rich  
17 PDEA is more hydrophilic than atactic PDEA. Thus, the tacticity is a key factor for the  
18 thermoresponsive behavior of PDEA. We demonstrated the effect of the tacticity on the phase  
19 separation dynamics for PDEA and showed that the phase separation rate for PDEA can be  
20 controlled by modifying the tacticity.

## 21 22 23 24 25 26 27 28 29 30 31 32 33 34 35 36 37 38 39 40 41 42 43 44 45 46 47 **Experimental Section**

### 48 49 50 **Materials.**

51  
52  
53 *N,N*-dimethylformamide (DMF), acetone, and *n*-hexane were purchased from Nacalai tesque.  
54  
55 Scandium(III) triflate (Sc(OTf)<sub>3</sub>) and Ytterbium(III) triflate (Y(OTf)<sub>3</sub>) were purchased from  
56  
57  
58  
59  
60

1  
2  
3 Aldrich. Dimethyl sulfoxide- $d_6$  (DMSO- $d_6$ ) was purchased from Tokyo Chemical Industries. All  
4 these reagents were used as received. *N,N*-diethyl acrylamide (DEA) was purchased from Tokyo  
5 Chemical Industries and distilled under reduced pressure at 90 °C to remove the inhibitor.  
6  
7 Methanol (special grade) and toluene (special grade) were purchased from Nacalai tesque and  
8 Wako Pure Chemical Industries, respectively, and they were distilled before use.  $\alpha,\alpha$ -  
9 azobis(isobutyronitrile) (AIBN) was purchased from Wako Pure Chemical Industries and was  
10 recrystallized from methanol. 1-Phenylethyl phenyldithioacetate (PEPD) was synthesized and  
11 identified according to the literature.<sup>35</sup>  
12  
13  
14  
15  
16  
17  
18  
19  
20  
21

### 22 **Synthesis of Stereo-Controlled PDEA.**

23  
24  
25 PDEA was synthesized by reversible addition-fragmentation chain transfer (RAFT)  
26 polymerization in the presence of a Lewis acid catalyst.<sup>43</sup> DEA (3.3 g, 26 mmol) as a monomer,  
27 PEPD as a RAFT agent, AIBN as an initiator, and Sc(OTf)<sub>3</sub> or Y(OTf)<sub>3</sub> as a Lewis acid catalyst  
28 were all dissolved in a methanol/toluene mixture (1:1, v:v, 10 mL) (with a molar feed ratio of  
29 [DEA]/[PEPD]/[AIBN] = 1500/3/1). Polymerization was carried out at 60 °C under a nitrogen  
30 ambient (polymerization time = 8.0 h). These polymers were purified twice by reprecipitation  
31 from acetone to *n*-hexane. The tacticity of PDEA was controlled by changing the concentration  
32 of the Lewis acid catalyst (0–0.14 M).  
33  
34  
35  
36  
37  
38  
39  
40  
41  
42  
43

### 44 **Sample Characterization.**

45  
46  
47 The weight-averaged molecular weight ( $M_w$ ) and the polydispersity ( $M_w/M_n$ ) of the PDEA  
48 samples were evaluated using size-exclusion chromatography (SEC) (Shimadzu system)  
49 equipped with a GPC K-806M column (Shodex). DMF (LiBr 10 mM) was used as an eluent with  
50 a flow rate of 1.0 mL min<sup>-1</sup> at 40 °C. SEC chromatograms were calibrated using standard  
51  
52  
53  
54  
55  
56  
57  
58  
59  
60

1  
2  
3 polystyrene samples (Tosoh Co., TSKgel). The concentration of the sample solutions was 10 mg  
4 mL<sup>-1</sup>. <sup>1</sup>H NMR spectra were recorded on a JEOL JNM-ECZ400S (400 MHz) in DMSO-*d*<sub>6</sub> at 130  
5  
6 °C to determine the tacticity of the samples (meso-diad content). The cloud point (*T*<sub>c</sub>) of the  
7  
8 sample solutions was determined on the basis of the temperature dependence of the optical  
9  
10 transmittance.<sup>40</sup> Temperature-variable dynamic light scattering (DLS) by the sample solutions  
11  
12 (0.10 wt%) was measured using an ELSZ-2000ZS (Otsuka Electronics Co.). The sample  
13  
14 solutions were filtered (Advantec, 13CP045AS, pore size: 0.45 μm) before the DLS experiments.  
15  
16  
17 The data were analyzed by the CONTIN algorithm.  
18  
19  
20

### 21 22 **Laser T-jump Technique Combined with Transient Photometry.**

23  
24  
25 Details of the laser T-jump technique have previously been described elsewhere and are briefly  
26  
27 introduced here.<sup>40</sup> The sample solutions were kept at a temperature marginally lower (0.20–1.0  
28  
29 K) than *T*<sub>c</sub> using a temperature controller and were irradiated with a single pulse of near-infrared  
30  
31 nanosecond laser light ( $\lambda = 1200$  nm), which was obtained by focusing a single 1064 nm laser  
32  
33 pulse (fwhm  $\approx 10$  ns) into a Raman shifter (Ba(NO<sub>3</sub>)<sub>2</sub> crystal) in an optical cavity. The laser  
34  
35 irradiation transiently induced phase separation (temperature rise;  $\Delta T = 1$ –1.5 K) by direct  
36  
37 vibrational excitation of the water molecules. For the probe light, a continuous-wave green laser  
38  
39 beam ( $\lambda = 532$  nm) was coaxially introduced into the solutions with the heating light pulse.  
40  
41  
42 Transient changes in the optical transmittance of the probe light were monitored by the increase  
43  
44 in turbidity of the solutions (due to the phase separation). The origin of the time scale ( $t = 0$ ) is  
45  
46 defined as the time when the heating pulse reaches the cell.  
47  
48  
49  
50  
51  
52  
53  
54

### 55 **Results and Discussion**



### Characterization of the Samples.

The fundamental characteristics of the synthesized PDEA are summarized in **Table 1**. The molecular weights of these lie in a narrow range ( $M_w = 60000\text{--}74000\text{ g mol}^{-1}$ ) with a low polydispersity index ( $M_w/M_n = 1.1\text{--}1.4$ ), which allowed us to easily investigate the effects of the tacticity (**Figure S1** in the Supporting Information shows SEC traces of all samples). The meso-diad content ( $m$ ) of the PDEAs ranged from 55 % to 90 %, determined from the methylene proton peaks of the polymer in the  $^1\text{H}$  NMR spectra (see the details in the Supporting Information, **Figure S2**).<sup>43</sup> We denoted the PDEAs on the basis of the value of  $m$  (e.g., “ $m55$ ” means PDEA with 55 % of  $m$ ). Note that,  $m55$  is an atactic PDEA, and the others are stereo-controlled (isotactic-rich) PDEA. The value of  $T_c$  in the aqueous PDEA solution increased from about 30 °C to 40 °C with increasing values of  $m$  ( $m55$  to  $m90$ ), indicating that the isotactic-rich PDEA was more hydrophilic than the atactic PDEA (**Figure S3** and **S4**). Such behavior is consistent with a report by Katsumoto and co-workers.<sup>43</sup>

**Table 1.** Characterization of synthesized PDEAs.

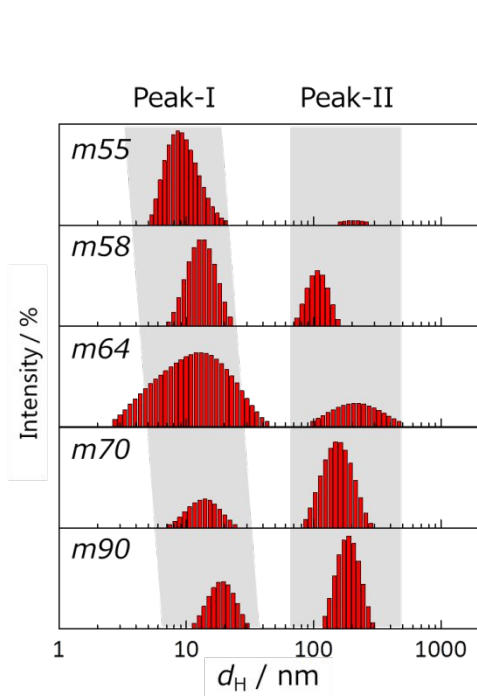
Entry	Name	$M_w$ <sup>a)</sup>	$M_w/M_n$ <sup>a)</sup>	$m:r$ <sup>b)</sup>	$T_c$ [°C] <sup>c)</sup>
1	$m55$	66000	1.4	55:45	31.1
2	$m58$	60000	1.1	58:42	32.4
3	$m64$	66000	1.2	64:36	33.4
4	$m70$	71000	1.4	70:30	34.0
5	$m90$	74000	1.1	90:10	39.9

<sup>a)</sup> Determined by SEC in DMF containing 10 mM LiBr at 40 °C (polystyrene standards).; <sup>b)</sup> Determined by  $^1\text{H}$ -NMR spectra of each sample in DMSO- $d_6$  at 130 °C.; <sup>c)</sup> Determined by the

1  
2  
3 transmittance curve. The sample concentration was 0.50 wt% and the heating rate was 0.2  
4 °C/min.  
5  
6  
7

### 8 9 **DLS Measurements.**

10  
11  
12 **Figure 1** shows the hydrodynamic diameter ( $d_H$ ) distribution for each sample in water at room  
13 temperature (polymer concentration was 0.10 wt%). We can clearly see two peaks in all these  
14 histograms. As in our previous work, the peak at smaller  $d_H$  (Peak-I) corresponds to individual  
15 single polymer chains, and the peak at larger  $d_H$  (Peak-II) is ascribed to polymer aggregates (pre-  
16 aggregates) arising from weak intermolecular interactions, such as the entanglement of polymer  
17 chains.<sup>40</sup> The average value of  $d_H$  for Peak-I increases from 10 nm to 19 nm with increasing  
18 isotacticity. This suggests that individual PDEA chains with higher isotacticity have relatively  
19 loose structures below  $T_c$  due to the sufficiently high level of hydration (higher hydrophilicity)  
20 compared with the lower isotacticity sample, which is in good agreement with the effect of the  
21 tacticity on  $T_c$ . This can be ascribed to the difference in the excluded volume effect in the  
22 polymer chains based on steric hindrance.<sup>44</sup> On the other hand, the average value of  $d_H$  for Peak-  
23 II is around 100–200 nm. The relative scattering intensity of Peak-II increases with increasing  
24 isotacticity, meaning that the number of pre-aggregates had increased. Note that, there was no  
25 effect due to the tacticity found in the values of  $d_H$  for Peak-II.  
26  
27  
28  
29  
30  
31  
32  
33  
34  
35  
36  
37  
38  
39  
40  
41  
42  
43  
44  
45  
46  
47  
48  
49  
50  
51  
52  
53  
54  
55  
56  
57  
58  
59  
60



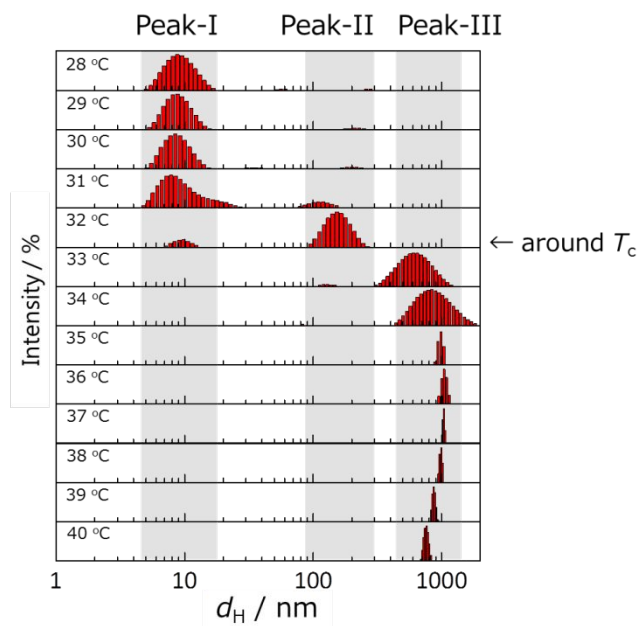
24  
25  
26  
27  
28  
29  
30  
31  
32

**Figure 1.** The  $d_H$  distributions for each PDEA, which have different tacticity, obtained by DLS experiments at room temperature. The polymer concentration was 0.10 wt%.

33  
34  
35  
36  
37  
38  
39  
40  
41  
42  
43  
44  
45  
46  
47  
48  
49  
50  
51  
52  
53  
54  
55  
56  
57  
58  
59  
60

**Figure 2** shows the temperature dependence of the  $d_H$  distributions for *m55* in water (polymer concentration was 0.10 wt%). In the histograms, we see three kinds of peaks: Peak-I (around 10 nm), Peak-II (from several tens of nanometers to a few hundred of nanometers), and Peak-III (around 1000 nm). Peak-I and Peak-II have already been described above in Figure 1. Peak-III is assigned to polymer-rich domains formed by phase separation. Below  $T_c$ , (25–30 °C), Peak-I and Peak-II are observed. The scattering intensity of Peak-II is significantly lower than that of Peak-I, meaning that there are hardly any pre-aggregates of PDEA in this temperature range. From 31 °C to 33 °C (around  $T_c$ ), the scattering intensity of Peak-I decreases while that of Peak-II increases. When Peak-I had almost completely disappeared at 33 °C, Peak-III appears due to the phase separation. Above  $T_c$  (34–40 °C), only one peak (Peak-III) can be observed. The

1  
2  
3 value of  $d_H$  for Peak-III increases slightly with increasing solution temperature up to 36 °C due  
4 to further aggregation and then gradually decreases. Such behavior above 36 °C suggests that the  
5 polymer-chain globules in the aggregates had become more compact.<sup>22</sup> Peak-I, Peak-II, and  
6 Peak-III were observed also in isotactic-rich PDEA (*m70*, **Figure S5** in the Supporting  
7 Information). The size of the aggregate after phase separation for *m70* was somewhat larger than  
8 that for *m55*. This might be due to that the aggregate of highly isotactic PDEA has more water  
9 than that for atactic PDEA because of higher hydrophilicity (higher  $T_c$ ). However, details are not  
10 discussed here. The corresponding correlation curves, which are raw-data in DLS experiments,  
11 were shown in **Figure S6** in the Supporting Information.



51 **Figure 2.** Temperature dependence of the  $d_H$  distributions for *m55* obtained by DLS  
52 experiments. The polymer concentration was 0.10 wt%. The waiting time after raising the  
53 temperature was 2 min.

### Phase Separation Dynamics for Stereo-Controlled PDEA.

**Figure 3** shows a representative transient decay curve of the optical transmittance obtained from the laser T-jump experiment (*m55*, 3.0 wt%), in which initial temperature was 29.2 °C ( $T_c$  was 29.7 °C). Immediately after the laser T-jump ( $t = 0$  s), the optical transmittance rapidly decays from 100 % to 25 % in  $t = 200$  ms due to the phase separation. After  $t = 200$  ms, the optical transmittance gradually recovers and it finally reached 100 % at about  $t = 1$  s because of cooling of the irradiated area in the sample solution. The decay curve was well fitted with a double exponential function,<sup>40</sup>

$$T(t) = A_{\text{fast}} \exp\left(-\frac{t}{\tau_{\text{fast}}}\right) + A_{\text{slow}} \exp\left(-\frac{t}{\tau_{\text{slow}}}\right) + B, \quad (1)$$

where  $\tau_{\text{fast}}$  and  $\tau_{\text{slow}}$  are time constants for the fast and slow phase separation, respectively.  $A_{\text{fast}}$  and  $A_{\text{slow}}$  are pre-exponential factors.  $B$  is a fitting constant corresponding to the minimum transmittance after the T-jump. Here, we define

$$f = \frac{A_{\text{fast}}}{A_{\text{fast}} + A_{\text{slow}}} \quad (2)$$

as the relative contribution of the fast phase separation component to the whole process. For Figure 3, we determined these parameters to be:  $\tau_{\text{fast}} = 8.3$  ms,  $\tau_{\text{slow}} = 54$  ms and  $f = 0.42$ .

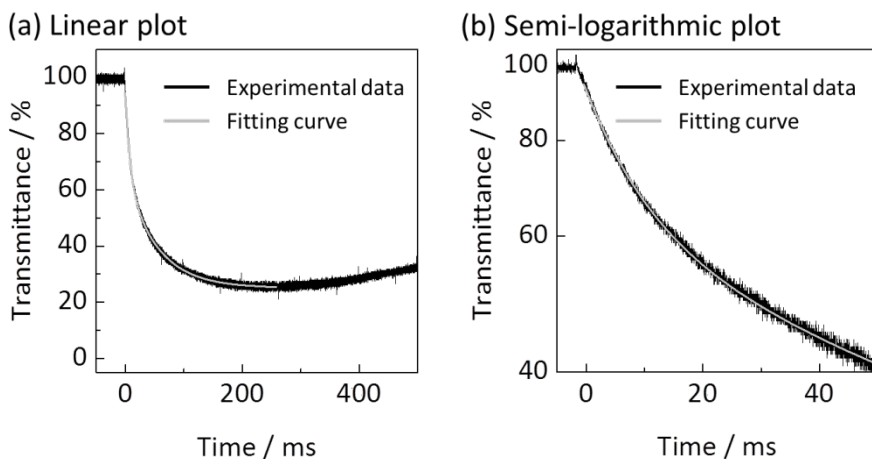


**Figure 3.** Representative transmittance curve (*m55*, 3.0 wt%). The origin of the time scale ( $t = 0$  s) is the time when the heating pulse reaches the sample cell. The initial temperature before the T-jump was 29.2 °C ( $T_c$  was 29.7 °C). The black lines show the experimental data. The gray line is the curve with a double exponential function fitted to the data ( $R^2 > 0.99$ ). (a) and (b) are linear and semi-logarithmic plots, respectively (same data).

In our previous study, we determined time constants of the phase separation for atactic PDEA and revealed that PDEA had two phase separation processes: a fast and a slow process.<sup>40</sup> We briefly describe the phase separation mechanism as follows. In the slow phase separation process, individual polymer chains (polymer globules) aggregate with each other by diffusion in solution. This is the normal phase separation process described in the introduction. In the fast phase separation process, the pre-aggregates undergo shrinkage accompanied by dehydration (coil-to-globule phase transition) without further aggregation. This causes an increase in refractive index because of an increase in averaged chain density and a decrease in water content.<sup>45</sup> Thus it should lead an increase in multiple light scattering resulting in a decrease of the light transmission. Such shrinkage behavior for physically crosslinked aggregates is similar

1  
2  
3 to the volume phase transition for chemically cross linked microgels in terms of time scale.  
4  
5 However, details are not discussed here.<sup>46</sup> Note that, aggregation of each pre-aggregate would  
6  
7 have negligible effects on the dynamics, because number of the pre-aggregates is significantly  
8  
9 lower than that of individual polymer chains (less than 1%).  
10  
11

12  
13 In the present study, we obtained  $\tau_{\text{fast}}$ ,  $\tau_{\text{slow}}$ , and  $f$  for both atactic PDEA and isotactic-rich  
14  
15 PDEA. As a representative example for isotactic-rich PDEA, the values for *m70* are plotted  
16  
17 against polymer concentration (0.50–10.0 wt%) in **Figure 4**.  $\tau_{\text{slow}}$  decreases from 110 ms to 20  
18  
19 ms with increasing polymer concentration, meaning that the slow phase separation process  
20  
21 accelerates as the concentration is increased. On the other hand, the time constant for the fast  
22  
23 process due to the pre-aggregates ( $\tau_{\text{fast}}$ ) remains at almost 10 ms irrespective of the polymer  
24  
25 concentration. Note that the  $f$  values of all the samples are around 0.4 (0.23–0.69) irrespective of  
26  
27 the concentration (Figure 4b), indicating that both the fast and slow processes make comparable  
28  
29 contributions to the whole phase separation process. That is, the slow process is the rate-  
30  
31 controlling step for the whole process. The concentration dependence of  $\tau_{\text{fast}}$ ,  $\tau_{\text{slow}}$ , and  $f$  for  
32  
33 atactic PDEA and other isotactic-rich PDEA are shown in **Figure S8** and **S9** in the Supporting  
34  
35 Information. In the next section, we describe the effect of the tacticity on the phase separation  
36  
37 dynamics for stereo-controlled PDEA.  
38  
39  
40  
41  
42  
43  
44  
45  
46  
47  
48  
49  
50  
51  
52  
53  
54  
55  
56  
57  
58  
59  
60

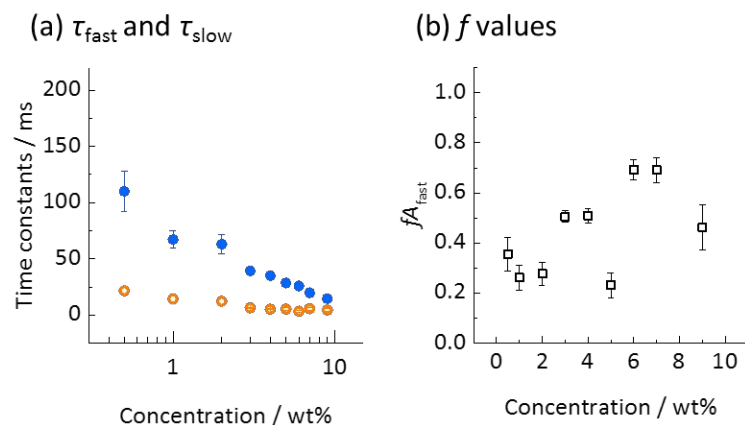


**Figure 4.** Dependences of the phase separation dynamics on concentration for *m70* (0.50–10 wt%). (a) The fast and slow time constants for the phase separation ( $\tau_{fast}$  and  $\tau_{slow}$ ). (b) The relative contribution of the fast phase separation component ( $f$ ). The orange open and blue closed circles show the average values of  $\tau_{fast}$  and  $\tau_{slow}$ , respectively. The black squares show the  $f$  value. The data were obtained by averaging over 30 laser T-jump experiments. The error bars show standard deviations.

### Effect of Tacticity on the Phase Separation Dynamics.

To discuss the effect of the tacticity on the dynamics,  $\tau_{fast}$  and  $\tau_{slow}$  are plotted against the value of  $m$  of the samples in **Figure 5**, where the polymer concentrations are (a) 10 wt% and (b) 0.50 wt%. In the 10 wt% solution,  $\tau_{slow}$  has little dependence upon the tacticity with  $\tau_{slow} \approx 23$  ms on average (Figure 5a). Wintgens and Amiel reported that polymer chains of both PNIPAM and its derivatives formed physical networks like hydrogels in highly concentrated aqueous solutions around  $T_c$ .<sup>47</sup> Therefore, the phase separation dynamics for PDEA in the dense solution (10 wt%) can be understood using a theory for the volume phase transition of hydrogels, which is in good agreement with previous PNIPAM systems.<sup>48</sup> According to the Tanaka-Fillmore theory, the rate



1  
2  
3 of such swelling or shrinkage is proportional to the inverse of the cooperative diffusion  
4 coefficient that depends on the cross linking density of the polymer network: that is, the polymer  
5 concentration.<sup>49,50</sup> Note that the tacticity of the polymer chains has no relationship with the  
6 average cross linking density in the solution. In the dilute solution (0.50 wt%),  $\tau_{\text{slow}}$  decreases  
7 from 250 ms to 80 ms as the value of  $m$  rises by 9%, and then remains constant with further  
8 increases in  $m$  (Figure 5b). Such behavior can be explained in terms of diffusion-controlled  
9 aggregation because the PDEA chains are homogeneously dissolved in water without  
10 intermolecular overlapping of the polymer chains in the dilute solution. This will be discussed in  
11 the later section. It is notable that higher temperature in isotactic-rich PDEA when the T-jump  
12 was applied had negligible effect on the dynamics, because the diffusion coefficient for each  
13 PDEA hardly depended on the temperature below the  $T_c$  (Figure S7 in the Supporting  
14 Information). Contrary to the slow process, the dynamics of the fast process are independent of  
15 the tacticity at any concentration ( $\tau_{\text{fast}} \approx 10$  ms). In other words, a number of pre-aggregate was  
16 hardly reflected in the fast process. This is consistent with the mechanism where the fast phase  
17 separation for PDEA is originated from the shrinkage of the pre-aggregates without any further  
18 diffusion-aggregation. What is important point here is that the slow phase separation that is  
19 dominant in the whole system accelerated by modification of the tacticity.  
20  
21  
22  
23  
24  
25  
26  
27  
28  
29  
30  
31  
32  
33  
34  
35  
36  
37  
38  
39  
40  
41  
42  
43  
44  
45  
46  
47  
48  
49  
50  
51  
52  
53  
54  
55  
56  
57  
58  
59  
60

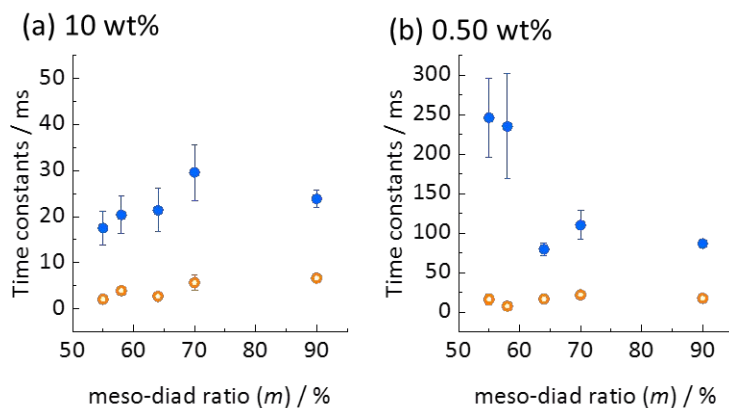


**Figure 5.** Effect of tacticity on  $\tau_{fast}$  and  $\tau_{slow}$  for PDEA. The polymer concentrations are (a) 10 wt% and (b) 0.50 wt%. The orange open and blue closed circles show the average values of  $\tau_{fast}$  and  $\tau_{slow}$ , respectively. The data were obtained by averaging over 30 laser T-jump experiments. The error bars show standard deviations.

### Stepwise Growth Model.

As described above, the phase separation for isotactic-rich PDEA was faster than that for atactic PDEA in the low concentration region. To understand the phase separation dynamics for this, we made a rough estimate of the growth rate of the polymer-rich domains using a stepwise (sequential) growth model based on diffusion-controlled aggregation.<sup>51</sup> **Figure 6a** shows a schematic illustration of this model. The calculation is based on the following assumptions: (1) in a dilute solution the domains grow by the collisions between a couple of adjacent polymer aggregates, (2) the mean square displacement of the aggregates is regarded as the average intermolecular distance between adjacent aggregates, and (3) the volume of the domain is equal to the sum of the volume of these two aggregates.

The diffusion time required for aggregation of the  $i^{\text{th}}$  step ( $t_i$ ) is expressed by equation (3), which is derived from the Stokes-Einstein equation.<sup>52,53</sup>

$$t_i = \frac{3 \pi \mu r_i^2}{4 k_B T d_{\text{agg},i}} \quad (3)$$

where  $k_B$  is the Boltzmann constant,  $T$  is absolute temperature,  $\mu$  is the viscosity of the solvent and  $d_{\text{agg},i}$  is the hydrodynamic diameter of a polymer aggregate,  $r_i$  is the diffusion distance, and  $t_i$  is the time required for the diffusion. The subscript “ $i$ ” means the  $i^{\text{th}}$  step.

$r_i$  was calculated as the average intermolecular distance between two adjacent aggregates, and thus is given by

$$r_i = \frac{d_{\text{agg},i_3}}{d_{\text{glo}}} \sqrt{\frac{M_w}{C_{\text{poly}} N_A}} \quad (\text{when } i = 1, d_{\text{agg},i} = d_{\text{glo}}) \quad (4)$$

where  $d_{\text{glo}}$  is the hydrodynamic diameter of a single polymer globule,  $C_{\text{poly}}$  is the concentration by weight of the polymer, and  $N_A$  is Avogadro’s number. According to the literature, PDEA chains with hydrated random-coil structures shrink by about 50 % after the phase transition.<sup>29</sup> Thus, we estimated the values of  $d_{\text{glo}}$  from the values of  $d_H$  obtained in the DLS measurements (Figure 1); for instance,  $d_{\text{glo}}$  for *m55* was 5 nm.

Combining equations (3) and (4), we obtained  $t_i$  for each step. As an example, we plot  $d_{\text{agg}}$  vs. total time ( $t = \sum t_i$ ) for *m55* in **Figure 6b**.  $d_{\text{agg}}$  increases step-by-step with time. Here, we assumed that our laser T-jump system monitored the time when the diameter of the domains became about 200 nm ( $\tau_{\text{cal}}$ ) by taking into account the effect of the particle size on the optical transmittance in solution, which is based on our preliminary experiment (see details in the Supporting Information, **Figure S10**). Based on this assumption, we obtained  $\tau_{\text{cal}}$  for all samples (0.50 wt%). All of the estimated values ( $\tau_{\text{cal}}$ ) and experimental values  $\tau_{\text{slow}}$  are summarized in

1  
2  
3 **Table 2.**  $\tau_{cal}$  decreases with increasing isotacticity from 250 ms to 90 ms and is close to  $\tau_{slow}$ .  
4  
5 Moreover, a number of collisions of polymer globules decreased with increasing the isotacticity.  
6  
7 The most important point in our model is that the phase separation dynamics for the stereo-  
8 controlled PDEA can be explained by the hydrophobicity that is reflected in the size of polymer  
9 chains. Note that difference in diffusion coefficient for the stereo-controlled PDEA has a  
10 negligible effect on the whole phase separation dynamics. Except for 0.50 wt%, our diffusion-  
11 limited aggregation model hardly explained the dynamics in the highly concentrated polymer  
12 solution (e.g. 10 wt%). This should be due to the non-negligible overlapping effect of the  
13 polymer chains because the overlap concentration of the synthesized PDEA is about 1-2 wt%. It  
14 is notable that our model is inappropriate for  $\tau_{fast}$  because the fast process does not need any  
15 further diffusion of the polymer chains. Altogether, we have thus successfully explained the  
16 mechanism that governs the acceleration in the phase separation of stereo-controlled PDEA  
17 using a simple model based on stepwise aggregation of the polymer chains.  
18  
19  
20  
21  
22  
23  
24  
25  
26  
27  
28  
29  
30  
31  
32  
33  
34  
35  
36  
37  
38  
39  
40  
41  
42  
43  
44  
45  
46  
47  
48  
49  
50  
51  
52  
53  
54  
55  
56  
57  
58  
59  
60

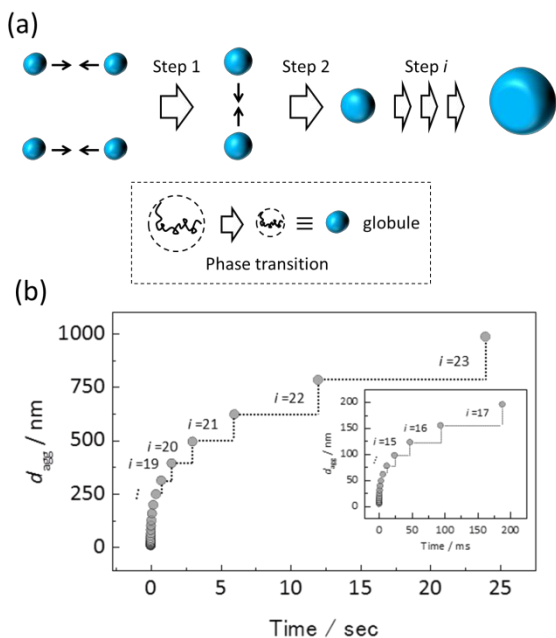


**Figure 6.** Stepwise Growth Model of a polymer-rich domain based on diffusion-limited aggregation of the polymer chains. (a) An illustration of the model. (b) Estimated growth-rate of a polymer-rich domain for *m55*. The inset shows an expanded view ranging from 0 ms to 200 ms.

**Table 2.** Summary of  $\tau_{\text{cal}}$  and  $\tau_{\text{slow}}$  for each sample.

	$\tau_{\text{cal}} / \text{ms}$ <sup>a)</sup>		$\tau_{\text{slow}} / \text{ms}$ <sup>b)</sup>
<i>m55</i>	190	( <i>i</i> = 17)	250
<i>m58</i>	120	( <i>i</i> = 16)	190
<i>m64</i>	130	( <i>i</i> = 16)	80
<i>m70</i>	76	( <i>i</i> = 15)	110
<i>m90</i>	50	( <i>i</i> = 14)	90

1  
2  
3 a) The growth rate of the PDEA-rich domain (the time when the domain became about 200 nm)  
4 estimated by a stepwise growth model based on diffusion-limited aggregation.; b) The time  
5 constant for slow phase separation of PDEA at 0.50 wt% determined by the laser T-jump  
6 experiments.  
7  
8  
9  
10

## 11 **Summary and Conclusions**

12  
13  
14  
15 In summary, in this study we investigated the dependence of the phase separation dynamics of  
16 aqueous PDEA solutions on the tacticity of the PDEA. According to the cloud point and DLS  
17 measurements, the hydrophobicity of PDEA decreases as the meso-diad ratio in the polymer  
18 chains increases, by which the hydrodynamic diameter becomes larger. In the laser T-jump  
19 experiments for the dynamics, it was found that atactic and isotactic-rich PDEA have fast phase  
20 separation processes (10 ms) in addition to the slow (normal) processes (80–250 ms). The fast  
21 process is ascribed to the polymer aggregates formed even below the cloud point and is  
22 independent of the tacticity. The slow process strongly depends on the tacticity. The phase  
23 separation of highly isotactic PDEA is clearly faster than that of atactic PDEA (maximum  
24 acceleration of 2.5 times) in the dilute solution. We used a stepwise growth model for polymer  
25 aggregates to successfully demonstrate that the acceleration of the slow phase separation process  
26 originates from the difference in the hydrophobicity of the PDEA.  
27  
28  
29  
30  
31  
32  
33  
34  
35  
36  
37  
38  
39  
40  
41  
42

43 In conclusion, we can control the phase separation in PDEA by a slight modification of  
44 the tacticity in a dilute solution. This new insight shows that the sum of the small differences in  
45 the static properties derived from the primary structure (chemical structure and stereoregularity)  
46 have a strong effect on the dynamics. We hope that the present study will help to provide an  
47 understanding of this complex phase separation behavior.  
48  
49  
50  
51  
52  
53  
54  
55  
56  
57  
58  
59  
60

1  
2  
3  
4  
5 ASSOCIATED CONTENT  
6  
7

8 **Supporting Information.**  
9

10 Supporting data includes additional fundamental data about the synthesized polymers and other  
11 plots of the phase separation dynamics. This material is available free of charge via the Internet  
12 at <http://pubs.acs.org>.  
13  
14  
15

16  
17 AUTHOR INFORMATION  
18

19  
20 **Corresponding Author**  
21

22  
23 twoboys@sci.osaka-cu.ac.jp (Y. T.)  
24  
25

26 **Author Contributions**  
27

28  
29 M. M conducted all experiments and wrote the manuscript. Y. T. conceived and supervised the  
30 project. All authors discussed the results and commented on the manuscript. All authors have  
31 given approval to the final version of the manuscript.  
32  
33  
34  
35

36  
37 **Notes**  
38

39  
40 The authors declare no competing financial interest.  
41  
42  
43  
44  
45

46 **ACKNOWLEDGMENTS**  
47  
48

49 This work was supported by JGC-S Scholarship Foundation, and JSPS KAKENHI Grant  
50 Numbers JP26288011, JP16K17922, and JP16H06506/JP16H06507 in Scientific Research on  
51  
52  
53  
54  
55  
56  
57  
58  
59  
60

1  
2  
3 Innovative Areas “Nano-Material Manipulation and Structural Order Control with Optical  
4 Forces”.  
5  
6  
7  
8  
9  
10

11  
12 **REFERENCES**  
13

- 14  
15 (1) Heskins, M.; Guillet, J. E. Solution Properties of Poly(N-isopropylacrylamide). *J.*  
16 *Macromol. Sci. Part A - Chem.* **1968**, *2* (8), 1441–1455.  
17  
18  
19  
20 (2) Fujishige, S.; Kubota, K.; Ando, I. Phase transition of aqueous solutions of poly (N-  
21 isopropylacrylamide) and poly (N-isopropylmethacrylamide). *J. Phys. Chem.* **1989**, *93*  
22 (4), 3311–3313.  
23  
24  
25  
26  
27  
28 (3) Wu, C.; Zhou, S. Thermodynamically Stable Globule State of a Single Poly(N-  
29 isopropylacrylamide) Chain in Water. *Macromolecules* **1995**, *28*, 5388–5390.  
30  
31  
32  
33 (4) Wang, X.; Qiu, X.; Wu, C. Comparison of the Coil-to-Globule and the Globule-to-Coil  
34 Transitions of a Single Poly(N-isopropylacrylamide) Homopolymer Chain in Water.  
35 *Macromolecules* **1998**, *31* (1), 2972–2976.  
36  
37  
38  
39  
40  
41 (5) Wu, C.; Wang, X. Globule-to-Coil Transition of a Single Homopolymer Chain in  
42 Solution. *Phys. Rev. Lett.* **1998**, *80*, 4092–4094.  
43  
44  
45  
46 (6) Cheng, H.; Shen, L.; Wu, C. LLS and FTIR studies on the hysteresis in association and  
47 dissociation of poly(N-isopropylacrylamide) chains in water. *Macromolecules* **2006**, *39*  
48 (6), 2325–2329.  
49  
50  
51  
52  
53  
54  
55  
56  
57  
58  
59  
60



- 1  
2  
3 (7) Kujawa, P.; Segui, F.; Shaban, S.; Diab, C.; Okada, Y.; Tanaka, F.; Winnik, F. M. Impact  
4 of end-group association and main-chain hydration on the thermosensitive properties of  
5 hydrophobically modified telechelic poly(N-isopropylacrylamides) in water.  
6  
7  
8  
9  
10 *Macromolecules* **2006**, *39* (1), 341–348.  
11  
12  
13 (8) Maeda, Y.; Higuchi, T.; Ikeda, I. Change in Hydration State during the Coil–Globule  
14 Transition of Aqueous Solutions of Poly(N-isopropylacrylamide) as Evidenced by FTIR  
15 Spectroscopy. *Langmuir* **2000**, *16* (c), 7503–7509.  
16  
17  
18  
19  
20  
21 (9) Plamper, F. a; Steinschulte, A. a; Hofmann, C. H.; Drude, N.; Mergel, O.; Herbert, C.;  
22 Erberich, M.; Schulte, B.; Winter, R.; Richtering, W. Toward Copolymers with Ideal  
23 Thermosensitivity: Solution Properties of Linear, Well-Defined Polymers of N-Isopropyl  
24 Acrylamide and N,N-Diethyl Acrylamide. *Macromolecules* **2012**, *45*, 8021–8026.  
25  
26  
27  
28  
29  
30  
31 (10) Winnik, F. M.; Regismond, S. T. A. Fluorescence methods in the study of the interactions  
32 of surfactants with polymers. *Colloids Surfaces A Physicochem. Eng. Asp.* **1996**, *118* (1–  
33 2), 1–39.  
34  
35  
36  
37  
38  
39 (11) Starovoytova, L.; Spěvák, J. Effect of time on the hydration and temperature-induced  
40 phase separation in aqueous polymer solutions. <sup>1</sup>H NMR study. *Polymer* **2006**, *47*, 7329–  
41 7334.  
42  
43  
44  
45  
46 (12) Spěvák, J.; Konefał, R.; Čadová, E. NMR Study of Thermoresponsive Block  
47 Copolymer in Aqueous Solution. *Macromol. Chem. Phys.* **2016**, *217*, 1370–1375.  
48  
49  
50  
51  
52  
53  
54  
55  
56  
57  
58  
59  
60

- 1  
2  
3 (13) Tiktopulo, E. I.; Bychkova, V. E.; Ricka, J.; Ptitsyn, O. B. Cooperativity of the Coil-  
4 Globule Transition in a Homopolymer: Microcalorimetric Study of Poly(N-  
5 isopropylacrylamide). *Macromolecules* **1994**, *27* (10), 2879–2882.  
6  
7  
8  
9  
10  
11 (14) Zhou, X.; Li, J.; Wu, C.; Zheng, B. Constructing the phase diagram of an aqueous solution  
12 of poly(n-isopropyl acrylamide) by controlled microevaporation in a nanoliter  
13 microchamber. *Macromol. Rapid Commun.* **2008**, *29*, 1363–1367.  
14  
15  
16  
17  
18 (15) Liu, P.; Song, L.; Li, N.; Lin, J.; Huang, D. Time dependence of phase separation enthalpy  
19 recovery behavior in aqueous poly(N-isopropylacrylamide) solution. *J. Therm. Anal.*  
20 *Calorim.* **2017**, *130* (2), 843–850.  
21  
22  
23  
24  
25  
26 (16) Meier-Koll, A.; Pipich, V.; Busch, P.; Papadakis, C. M.; Müller-Buschbaum, P. Phase  
27 separation in semidilute aqueous poly(N-isopropylacrylamide) solutions. *Langmuir* **2012**,  
28 *28* (23), 8791–8798.  
29  
30  
31  
32  
33  
34 (17) Stieger, M.; Pedersen, J. S.; Lindner, P.; Richtering, W. Are thermoresponsive microgels  
35 model systems for concentrated colloidal suspensions? A rheology and small-angle  
36 neutron scattering study. *Langmuir* **2004**, *20* (17), 7283–7292.  
37  
38  
39  
40  
41  
42 (18) Djokpé, E.; Vogt, W. N-isopropylacrylamide and N-isopropylmethacrylamide: Cloud  
43 points of mixtures and copolymers. *Macromol. Chem. Phys.* **2001**, *202* (5), 750–757.  
44  
45  
46  
47 (19) Qiu, Q.; Lou, A.; Somasundaran, P.; Pethica, B. A. Intramolecular association of  
48 poly(maleic acid/octyl vinyl ether) in aqueous solution. *Langmuir* **2002**, *18* (15), 5921–  
49 5926.  
50  
51  
52  
53  
54  
55  
56  
57  
58  
59  
60

- 1  
2  
3 (20) Idziak, I.; Avoce, D.; Lessard, D.; Gravel, D.; Zhu, X. X. Thermosensitivity of Aqueous  
4 Solutions of Poly(N,N-diethylacrylamide). *Macromolecules* **1999**, *32* (4), 1260–1263.  
5  
6  
7  
8 (21) Itakura, M.; Inomata, K.; Nose, T. Aggregation behavior of poly (N,N-diethylacrylamide)  
9 in aqueous solution. *Polymer* **2000**, *41*, 8681–8687.  
10  
11  
12  
13 (22) Shen, L.; Zhang, G. Formation of Mesoglobules By Poly (N,N-Diethylacrylamide ).  
14 *Chinese J. Polym. Sci.* **2009**, *27* (4), 561–567.  
15  
16  
17 (23) Maeda, Y.; Nakamura, T.; Ikeda, I. Change in Solvation of Poly(N,N-diethylacrylamide)  
18 during Phase Transition in Aqueous Solutions As Observed by IR Spectroscopy.  
19 *Macromolecules* **2002**, *35* (27), 10172–10177.  
20  
21  
22  
23 (24) Hashimoto, C.; Nagamoto, A.; Maruyama, T.; Kariyama, N.; Iriya, Y.; Ikehata, A.; Ozaki,  
24 Y. Hydration States of Poly(N-isopropylacrylamide) and Poly(N,N-diethylacrylamide)  
25 and Their Monomer Units in Aqueous Solutions with Lower Critical Solution  
26 Temperatures Studied by Infrared Spectroscopy. *Macromolecules* **2013**, *46*, 1041–1053.  
27  
28  
29 (25) Lu, Y.; Zhou, K.; Ding, Y.; Zhang, G.; Wu, C. Origin of hysteresis observed in  
30 association and dissociation of polymer chains in water. *Phys. Chem. Chem. Phys.* **2010**,  
31 *12*, 3188–3194.  
32  
33  
34 (26) Lessard, D. G.; Ousalem, M.; Zhu, X. X. Effect of the molecular weight on the lower  
35 critical solution temperature of poly(N,N-diethylacrylamide) in aqueous solutions. *Can. J.*  
36 *Chem.* **2001**, *79* (11), 1870–1874.  
37  
38  
39  
40  
41  
42  
43  
44  
45  
46  
47  
48  
49  
50  
51  
52  
53  
54  
55  
56  
57  
58  
59  
60

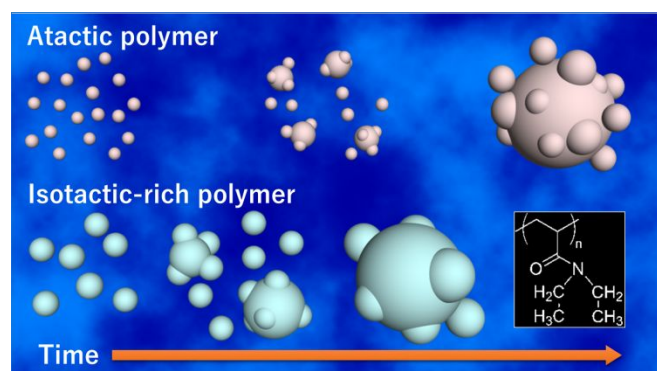
- 1  
2  
3 (27) Lessard, D. G.; Ousalem, M.; Zhu, X. X.; Eisenberg, A.; Carreau, P. J. Study of the phase  
4 transition of poly(n,n-diethylacrylamide) in water by rheology and dynamic light  
5 scattering. *J. Polym. Sci. Part B Polym. Phys.* **2003**, *41*, 1627–1637.  
6  
7  
8  
9  
10 (28) Katsumoto, Y.; Tanaka, T.; Ozaki, Y. Molecular interpretation for the solvation of  
11 poly(acrylamide)s. I. Solvent-dependent changes in the C=O stretching band region of  
12 poly(N,N-dialkylacrylamide)s. *J. Phys. Chem. B* **2005**, *109* (44), 20690–20696.  
13  
14  
15  
16  
17 (29) Zhou, K.; Lu, Y.; Li, J.; Shen, L.; Zhang, G.; Xie, Z.; Wu, C. The Coil-to-Globule-to-Coil  
18 Transition of Linear Polymer Chains in Dilute Aqueous Solutions: Effect of Intrachain  
19 Hydrogen Bonding. *Macromolecules* **2008**, *41* (22), 8927–8931.  
20  
21  
22  
23  
24 (30) Maeda, Y. Hydration of temperature-responsive polymers observed by IR spectroscopy.  
25 *Macromol. Symp.* **2011**, *303*, 63–70.  
26  
27  
28  
29  
30 (31) Strandman, S.; Lessard, D. G.; Van Dusschoten, D.; Wilhelm, M.; Wood-Adams, P. M.;  
31 Spiess, H. W.; Zhu, X. X. Two-dimensional Fourier transform rheological study on  
32 thermosensitivity of poly(N,N-diethylacrylamide) in aqueous solutions. *Polymer* **2012**, *53*  
33 (21), 4800–4805.  
34  
35  
36  
37  
38 (32) Lu, Y.; Ye, X.; Zhou, K.; Shi, W. A Comparative Study of Urea-Induced Aggregation of  
39 Collapsed Poly(N-isopropylacrylamide) and Poly(N,N-diethylacrylamide) Chains in  
40 Aqueous Solutions. *J. Phys. Chem. B* **2013**, *117*, 7481–7488.  
41  
42  
43  
44  
45 (33) Pang, X.; Cui, S. Single-chain mechanics of poly(N,N-diethylacrylamide) and poly(N-  
46 isopropylacrylamide): comparative study reveals the effect of hydrogen bond donors.  
47  
48  
49  
50  
51  
52  
53  
54  
55  
56  
57  
58  
59  
60

- 1  
2  
3 (34) Rembert, K. B.; Okur, H. I.; Hilty, C.; Cremer, P. S. An NH Moiety Is Not Required for  
4 Anion Binding to Amides in Aqueous Solution. *Langmuir* **2015**, *31* (11), 3459–3464.  
5  
6  
7  
8  
9 (35) Jia, D.; Zuo, T.; Rogers, S.; Cheng, H.; Hammouda, B.; Han, C. C. Re-entrance of  
10 Poly(N,N-diethylacrylamide) in D2O/d-Ethanol Mixture at 27 °C. *Macromolecules* **2016**,  
11 *49* (14), 5152–5159.  
12  
13  
14  
15  
16 (36) Termühlen, F.; Kuckling, D.; Schönhoff, M. Isothermal Titration Calorimetry to Probe the  
17 Coil-to-Globule Transition of Thermoresponsive Polymers. *J. Phys. Chem. B* **2017**, *121*  
18 (36), 8611–8618.  
19  
20  
21  
22  
23  
24 (37) Pagonis, K.; Bokias, G. Upper critical solution temperature-type cononsolvency of  
25 poly(N,N-dimethylacrylamide) in water-organic solvent mixtures. *Polymer* **2004**, *45* (7),  
26 2149–2153.  
27  
28  
29  
30  
31  
32 (38) Wu, M.; Zhang, H.; Liu, H. Study of phase separation behavior of poly (N,N-  
33 diethylacrylamide) in aqueous solution. *Polym. Bull.* **2018**, No. 0123456789.  
34  
35  
36  
37 (39) Tsuboi, Y.; Yoshida, Y.; Okada, K.; Kitamura, N. Phase separation dynamics of aqueous  
38 solutions of thermoresponsive polymers studied by a laser T-jump technique. *J. Phys.*  
39 *Chem. B* **2008**, *112* (i), 2562–2565.  
40  
41  
42  
43  
44  
45 (40) Matsumoto, M.; Wakabayashi, R.; Tada, T.; Asoh, T.-A.; Shoji, T.; Kitamura, N.; Tsuboi,  
46 Y. Rapid Phase Separation in Aqueous Solution of Temperature-Sensitive Poly(N,N-  
47 diethylacrylamide). *Macromol. Chem. Phys.* **2016**, *217* (23), 2576–2583.  
48  
49  
50  
51  
52  
53  
54  
55  
56  
57  
58  
59  
60

- 1  
2  
3 (41) Tsuchiizu, A.; Hasegawa, T.; Katsumoto, Y. Water sorption on a thin film of  
4 stereocontrolled poly(N-ethylacrylamide) and poly(N,N-diethylacrylamide). *MATEC Web*  
5  
6 *Conf.* **2013**, *4*, 1–4.  
7  
8  
9  
10  
11 (42) Kobayashi, M.; Ishizone, T.; Nakahama, S. Synthesis of highly isotactic poly(N,N-  
12 diethylacrylamide) by anionic polymerization with grignard reagents and diethylzinc. *J.*  
13 *Polym. Sci., Part A Polym. Chem.* **2000**, *38* (S1), 4677–4685.  
14  
15  
16  
17  
18 (43) Katsumoto, Y.; Etoh, Y.; Shimoda, N. Phase Diagrams of Stereocontrolled Poly(N,N-  
19 diethylacrylamide) in Water. *Macromolecules* **2010**, *43* (6), 3120–3121.  
20  
21  
22  
23  
24 (44) Kuznetsova, I. M.; Zaslavsky, B. Y.; Breydo, L.; Turoverov, K. K.; Uversky, V. N.  
25 Beyond the excluded volume effects: Mechanistic complexity of the crowded milieu.  
26  
27 *Molecules* **2015**, *20* (1), 1377–1409.  
28  
29  
30  
31  
32 (45) Garner, B. W.; Cai, T.; Ghosh, S.; Hu, Z.; Neogi, A. Refractive index change due to  
33 volume-phase transition in polyacrylamide gel nanospheres for optoelectronics and bio-  
34 photonics. *Appl. Phys. Express* **2009**, *2* (5), 2–5.  
35  
36  
37  
38  
39 (46) Keidel, R.; Ghavami, A.; Lugo, D. M.; Lotze, G.; Virtanen, O.; Beumers, P.; Pedersen, J.  
40 S.; Bardow, A.; Winkler, R. G.; Richtering, W. Time-resolved structural evolution during  
41 the collapse of responsive hydrogels: The microgel-to-particle transition. *Sci. Adv.* **2018**, *4*  
42 (4), 1–9.  
43  
44  
45  
46  
47  
48  
49 (47) Wintgens, V.; Amiel, C. Physical gelation of amphiphilic poly(N-isopropylacrylamide):  
50 Influence of the hydrophobic groups. *Macromol. Chem. Phys.* **2008**, *209* (15), 1553–1563.  
51  
52  
53  
54  
55  
56  
57  
58  
59  
60

- 1  
2  
3 (48) Wang, J.; Liu, B.; Ru, G.; Bai, J.; Feng, J. Effect of Urea on Phase Transition of Poly(N-  
4 isopropylacrylamide) and Poly(N,N-diethylacrylamide) Hydrogels: A Clue for Urea-  
5 Induced Denaturation. *Macromolecules* **2016**, *49*, 234–243.  
6  
7  
8  
9  
10  
11 (49) Tanaka, T.; Fillmore, D. J. Kinetics of swelling of gels. *J. Chem. Phys.* **1979**, *70* (3),  
12 1214–1218.  
13  
14  
15  
16 (50) Hirose, H.; Shibayama, M. Kinetics of Volume Phase Transition in Poly(N-  
17 isopropylacrylamide-co-acrylic acid) Gels. *Macromolecules* **1998**, *31* (16), 5336–5342.  
18  
19  
20  
21 (51) Lattuada, M. Predictive model for diffusion-limited aggregation kinetics of nanocolloids  
22 under high concentration. *J. Phys. Chem. B* **2012**, *116* (1), 120–129.  
23  
24  
25  
26  
27 (52) Einstein, A. Zur Theorie der Brownschen Bewegung. *Ann. Phys.* **2005**, *14* (S1), 248–258.  
28  
29  
30 (53) Sutherland, W. Dynamical Theory of Diffusion for Non-Electrolytes and the Molecular  
31 Mass of Albumin. *Philosophical Magazine*. 1905, pp 781–785.  
32  
33  
34  
35

36 Table of Contents.  
37  
38



56 **KEYWORDS:** LCST, poly(N,N-diethylacrylamide), globule, microgel, phase transition  
57  
58  
59  
60